

# Nanocomposite hybrids of cashew apple bagasse-derived lignin with photoprotective properties for sunscreen applications

**Tigressa Helena Soares Rodrigues**, Chemistry Course, Center of Exact Sciences and Technology, State University of Vale do Acaraú, Sobral, Brazil

**Gabriel Arcanjo Bezerra Matias, Vanessa Moreira Frota**, Department of Chemical Engineering, Federal University of Ceará, Fortaleza, Brazil

**Adriano L. A. Mattos**, Biomass Technology Laboratory, Empresa Brasileira de Pesquisa Agropecuária - Embrapa Tropical Agroindustry, Fortaleza, Brazil

**Maria Valdez Ponte Rocha**,  Department of Chemical Engineering, Federal University of Ceará, Fortaleza, Brazil

Received January 31 2025; Revised March 16 2025; Accepted March 24 2025;

View online at Wiley Online Library ([wileyonlinelibrary.com](http://wileyonlinelibrary.com));

DOI: 10.1002/bbb.2775; *Biofuels, Bioprod. Bioref.* (2025)



Abstract: Prolonged exposure to ultraviolet (UV) radiation can cause significant damage to the skin and immune system. There has consequently been an increasing emphasis on the development of biodegradable and sustainable materials that offer UV protection, reflecting increased awareness of health and disease prevention. Due to its high concentration of phenolic groups, lignin has emerged as a promising candidate for natural UV protective materials. This study therefore aimed to produce nanocomposites of lignin from cashew apple bagasse, due to its wide availability and high lignin content, combined with zinc or titanium oxides for sunscreen application. Fourier transform infrared (FTIR) spectroscopy and X-ray analysis confirm interactions between lignin and zinc/titanium oxides. The resulting nanocomposites are stable, as indicated by their zeta potential (−32 mV to −48 mV). Lignin nanocomposites (LigZnO and LigTiO<sub>2</sub>) exhibited similar antioxidant activity, though lower than that of lignin alone. Although lignin nanocomposites exhibited low sun protection factor (SPF) values in an emulsion base, they enhanced SPF in a commercial sunscreen. LigZnO (15.9) and LigTiO<sub>2</sub> (15.7) boosted the effectiveness of commercial UV absorbers (Parsol MCX and avobenzone), outperforming formulations with lignin alone or commercial ZnO and TiO<sub>2</sub>. The synergistic interaction between LigTiO<sub>2</sub>, LigZnO, and organic UV blockers reinforced thixotropy, making lignin nanocomposites a promising additive for sunscreen formulations. Their low cost and sustainable synthesis add value to nanomaterials while mitigating agro-waste disposal. © 2025 The Author(s). *Biofuels, Bioproducts and Biorefining* published by Society of Industrial Chemistry and John Wiley & Sons Ltd.

Supporting information may be found in the online version of this article.

Correspondence to: Maria Valdez Ponte Rocha, Department of Chemical Engineering, Federal University of Ceará, Av. Humberto Monte s/n, Fortaleza 60440-593, CE, Brazil. E-mail: [valdez.rocha@ufc.br](mailto:valdez.rocha@ufc.br)

Key words: lignin; cashew apple bagasse; sustainability; nanocomposites; UV-blockers; rheology

## Introduction

The cosmetic industry is among the fastest growing sectors globally. The global sun care market was valued at \$11.6 billion in 2018 and is projected to reach \$24.4 billion by 2029.<sup>1</sup> Increasing consumer demand for products containing natural compounds has heightened interest in identifying natural substances that can absorb ultraviolet (UV) radiation effectively.<sup>2,3</sup> Several studies reported in the literature, for example by Tafuro *et al.*,<sup>3</sup> Schneider and Lin,<sup>4</sup> and Xiao *et al.*<sup>5</sup> report that the use of natural polymers in cosmetic formulations is expanding, driven by a broader interest in sustainability and environmental concerns.

From an environmental perspective, organic filters used in sunscreens are considered harmful, as they contribute to coral reef bleaching and they accumulate in water supplies and aquatic organisms. Although no adverse effects on human health have been conclusively identified, ongoing research is being conducted in this area.<sup>4,6</sup> The use of sustainable, biodegradable UV absorbers, such as lignin, thus represents a promising alternative to conventional organic UV blockers.

Over the past two decades, lignin – a natural heterogeneous biopolymer that constitutes 15% to 30% w/w of agricultural biomass<sup>7</sup> – has gained recognition as a safe, biodegradable UV-protecting agent that can be used as a substitute for chemical UV absorbers.<sup>8</sup> Lignin possesses a broad natural spectrum of UV protection, along with antioxidant properties and effective antimicrobial activity.<sup>9</sup> Research efforts have focused on its application as an active ingredient in sunscreens, UV protective films, and other products. However, Zang *et al.*<sup>8</sup> reported that the dark brown color of lignin can limit its widespread use. Conversely, combining lignin with metal oxides to form hybrid nanocomposites can change lignin's color from dark brown to light brown, enhancing its applicability. Kaur *et al.*<sup>10</sup> and Kaur *et al.*<sup>11</sup> noted that the interactions between the organic component (lignin) and inorganic components (ZnO, TiO<sub>2</sub>) can improve the stability and synergies of the resulting hybrid nanomaterial.

Then, it is important to identify biomass sources that yield high lignin content within a biorefinery framework. In this context, this study evaluated cashew apple bagasse, which contains a high lignin content (33.0% to 35.5% w/w) as a byproduct of the cashew agroindustry.<sup>12,13</sup> Among the biopolymers in cashew apple bagasse, cellulose and hemicellulose are the most extensively studied for their potential to generate high-value products<sup>14</sup> such as xylitol<sup>15</sup>

and polylactic acid,<sup>16</sup> as well as biofuels like ethanol<sup>17</sup> and hydrogen through bioprocesses.<sup>18</sup> Developing processes for the application and valorization of lignin is therefore a primary concern, given the significant lignin content in cashew apple bagasse, its low cost, and the beneficial properties of this biopolymer.<sup>7</sup>

Based on these considerations, this study aimed to investigate a novel application of lignin derived from cashew apple bagasse as a UV absorber, in combination with zinc or titanium oxides. A green synthesis approach,<sup>10,11</sup> employing a nontoxic and renewable solvent, was used to incorporate it into commercial sunscreen formulations. The study aimed to evaluate the UV protection, compatibility, antioxidant activity, and rheological properties of the resulting formulations.

## Materials and methods

### Materials

All chemicals used in this investigation were of analytical grade or higher unless indicated otherwise. Methanol and ethanol were purchased from Êxodo Científica (São Paulo, Brazil). Zinc acetate dihydrate (Zn(C<sub>2</sub>H<sub>3</sub>O<sub>2</sub>)<sub>2</sub>·2H<sub>2</sub>O), titanium isopropoxide (Ti[OCH(CH<sub>3</sub>)<sub>2</sub>]<sub>4</sub>), zinc oxide (ZnO) nanoparticles, ascorbic acid (C<sub>6</sub>H<sub>8</sub>O<sub>6</sub>) and 2,2-diphenyl-1-picrylhydrazyl (DPPH) were purchased from Merck (Darmstadt, Germany). Titanium dioxide (TiO<sub>2</sub>) anatase nanoparticles were purchased from Yuanming Ruyun Technology Co. (Putian City, China). The body lotion was purchased from a local pharmaceutical manufacturer (Farmaformula Ltda, Ceará, Brazil).

### Lignin extraction and separation

The cashew apple bagasse (*Anacardium occidentale* L.) used in this work was obtained from the juice extraction process by peduncle pressing. The cashew apple bagasse (CAB) was preliminarily treated following a method described by Rodrigues *et al.*<sup>17</sup> The raw material was then submitted to acid-alkali pretreatment<sup>19</sup> to disrupt the intrinsic polysaccharide-lignin interactions efficiently and facilitate the extraction of the lignin. The lignin present in the liquid fraction was then recovered by acid precipitation as described by Serpa *et al.*<sup>12</sup> The lignin was ground and particles with a size smaller than 180 µm were selected. Then, the lignin was stored at room temperature (25 °C) to carry out the experiments.

## Preparation of the lignin-based nanocomposites with ZnO or TiO<sub>2</sub>

Lignin-hybrid nanocomposites with zinc oxide (LigZnO) or titanium dioxide (LigTiO<sub>2</sub>) were obtained by one-step synthesis with modifications of the methods proposed by Kaur *et al.*<sup>10</sup> and Kaur *et al.*<sup>11</sup> Initially, lignin (100 mg) was dissolved in 5 mL of 0.2 M NaOH for both nanocomposite preparations. The zinc-lignin nanocomposites were prepared using 24 mM zinc acetate dihydrate salt dissolved in ethanol for a reactional volume of 50 mL. Lignin solution (5 mL) was added dropwise into zinc acetate solution at 50 °C under stirred at 1000 rpm, and the reactional mixture was incubated for 24 h at 50 °C to synthesize the LigZnO nanocomposites. In the synthesis of titanium-lignin nanocomposites, lignin solution (5 mL) was diluted to 50 mL using ethanol followed by the addition of titanium isopropoxide (24 mM) dropwise at 70 °C and 1000 rpm. The reaction mixture was incubated for 24 h at 70 °C in the dark to synthesize the LigTiO<sub>2</sub> nanocomposites. Subsequently, pellets of both nanocomposites were homogenized at 15 000 rpm for 20 min using an Ultra-Turrax homogenizer (IKA, Staufen, Germany). The resulting mixture was then centrifuged at 5031 g for 20 min. The LigZnO and LigTiO<sub>2</sub> pellets were washed three times with ethanol and deionized water, respectively. Following this, the lignin-hybrid nanocomposites were dried at 100 °C for 24 h and stored at 25 °C. The yields of the nanocomposites (LigZnO and LigTiO<sub>2</sub>) were calculated by dividing the mass of the obtained nanocomposites by the total mass of the lignin and the precursor salts of zinc or titanium used.

## Nanocomposites characterization

The lignin and lignin-based nanocomposites were characterized initially using Fourier transform infrared spectroscopy (FTIR) and X-ray diffraction (XRD). Fourier transform infrared analyses were carried out on an FTIR Spectrum Two spectrometer (PerkinElmer, Hopkinton MA, USA) operating in the 4000–400 cm<sup>-1</sup> spectral range, with an average of 32 scans and 4 cm<sup>-1</sup> of spectral resolution. The XRD analysis was conducted using cobalt radiation and operation at 40 kV and 40 mA on a PANalytical X'Pert PRO diffractometer – model MDP (Malvern Instruments Ltd, Malvern, United Kingdom). Parallel beam geometry was used with a hybrid monochromator (mirror + Ge monochromator) and a 1/4° slit. The analysis was carried out using a spinner of 2 rps and the geometry of the diffracted beam consisted of a soller slit of 0.02°. A Bragg–Brentano scanning axis was used. The range was from 10° to 100°, with an angular step of 0.013° (2θ) and a time per step of

68.85 s, corresponding to a speed of 0.049°/s. Zeta potential and size data were collected from the nanocomposite pellets suspension and lignin at dilution of 1:100 in ultrapure water and sonicated for 10 min followed by analysis using Zetasizer Nano ZS90 (Malvern Instruments Ltd, Malvern, United Kingdom).

## Antioxidant and photoprotective properties (UV A/UV B correlation)

The antioxidant potential of lignin-based nanocomposites, and commercial nanoparticles of titanium (Yuanming Ruyun Technology Co) and zinc oxides (Merck) were determined using a 2,2-diphenyl-1-picrylhydrazyl (DPPH) assay. First, lignin, nanocomposites, and oxides solutions were prepared at 50 µg mL<sup>-1</sup> in methanol/ethanol (1:1). The positive control was ascorbic acid at 30 µg mL<sup>-1</sup> in the same solvent. The DPPH solution (0.14 mM) was prepared in methanol.<sup>10,11</sup> The sample solution (1.72 mL) was added to 0.28 mL of DPPH solution with vigorous shaking and incubated for 30 min at 27 °C in the dark. The experiments were conducted in triplicate and absorbance was recorded at 517 nm. The percentage scavenging by the nanocomposites (NCs) was calculated using Eqn (1):

$$\text{scavenging (\%)} = \frac{\text{Abs}_{\text{control}} - \text{Abs}_{\text{sample}}}{\text{Abs}_{\text{control}}} \times 100 \quad (1)$$

The ultraviolet-A and ultraviolet-B (UV A/UV B) ratio of the samples was determined by the ratio of the UV absorbance spectra area in the UV A (320–400 nm) and UV B (290–320 nm) region obtained from the lignin, nanocomposites and oxide solutions at a concentration of 200 µg mL<sup>-1</sup> in methanol/ethanol (1:1). The maximum UV absorption of samples was also determined in the range of 200–600 nm.

## Sunscreen preparations

The lotions used in this study included a commercial emulsion base without UV absorbers and a commercial sunscreen with a sun protection factor (SPF) of 12.6 ± 0.3, containing organic UV blockers – Parsol MCX (7% w/w) and avobenzene (3% w/w). These formulations were used to incorporate lignin, lignin-based nanocomposites (LigZnO and LigTiO<sub>2</sub>), and commercial oxides (ZnO and TiO<sub>2</sub>). Sunscreens containing 5% (w/w) of active ingredients (lignin, LigZnO, LigTiO<sub>2</sub>, ZnO, or TiO<sub>2</sub>) were dispersed homogeneously at 4000 rpm for 10 min using an Ultra-Turrax Tube Drive (IKA). The SPF values of the prepared sunscreens were determined using the spectrophotometry method.<sup>20–22</sup>

The formulations were solubilized in ethanol at 0.2 mg mL<sup>-1</sup> and the absorption data were obtained in the range of 290 to 320 nm (varying 5 nm), followed by the application of the Mansur equation (Eqn 2):

$$SPF_{\text{spectrophotometric}} = CF \times \sum_{290}^{320} EE(\lambda) \times I(\lambda) \times Abs(\lambda) \quad (2)$$

where *EE* is the erythemal effect spectrum; *I* is the solar intensity spectrum; *Abs* is the absorbance of sunscreen product; *CF* is the correction factor (= 10). The values of *EE* × *I* are constants and were determined by Sayre *et al.*<sup>23</sup> From SPF data, the UV boosting effect (BE) for sunscreen formulations was expressed as a percentage following Piccinino *et al.*<sup>24</sup>

## Rheological determinations

The rheological measurements were conducted using a controlled-stress rheometer (Haake Mars, Thermo Fisher Scientific, Waltham MA, USA) equipped with a cone-and-plate geometry (C35/2° TiL) at a constant temperature (25 °C). An oscillatory rheology experiment was performed at a frequency of 1 Hz for 4.00 min to determine the dynamic viscosity (*η*), storage modulus (*G'*), and loss modulus (*G''*) of the sunscreen formulations. Thixotropy measurements were carried out in a rotational experiment utilizing the same geometry. The shear rate was increased linearly from 0.001 to 450 s<sup>-1</sup>, and the areas representing thixotropy were calculated by integrating the areas between the 'up' and 'down' curves of the formulations studied.

## Results and discussion

### Characterization of lignin, LigZnO and LigTiO<sub>2</sub> nanocomposites

Table 1 summarizes the yields, λ<sub>max</sub>, UV A/UV B correlation, zeta potential, and size of lignin, LigZnO, LigTiO<sub>2</sub>. Regarding the lignin yield, Serpa *et al.*<sup>12</sup> reported 55.2 ± 2.2% w/w of lignin recovery from dry CAB under the same conditions

that were used in this study. This highlights that part of the total lignin from CAB also remains in the solids fractions along the pretreatment applied. Considering a range of 33% to 35% w/w lignin in cashew apple bagasse, this represents an available mass of 56 kg per ton of wet CAB (from the peduncle industrial process) for the LigZnO and LigTiO<sub>2</sub> nanocomposites production. The yields of nanocomposites were similar for LigZnO (37.2 ± 1.3% w/w) and LigTiO<sub>2</sub> (34.3 ± 2.2% w/w), based on the initial mass of lignin and salts of zinc or titanium applied.

The nanocomposites exhibited minimal variation in λ<sub>max</sub>: LigZnO matched lignin at 280 nm, and LigTiO<sub>2</sub> had a slightly higher λ<sub>max</sub> of 318 nm (Supporting Information, Fig. S1). The UV A/UV B correlation relates UV A to UV B absorption for a given photoprotector. If the rate is greater than 1, the absorption of UV A radiation by the UV absorber will be greater than the absorption of UV B radiation. Ideally, the UV A/UV B ratio should be near to 1 to provide broad-spectrum protection.<sup>25</sup> Lignin and the nanocomposites exhibited stronger photoprotection in the UV A region than in the UV B region. In the UV A region (315–400 nm), LigZnO and LigTiO<sub>2</sub> displayed better absorption than lignin, which can be confirmed by the UV A/UV B ratio values. Lignin-based nanocomposites consequently provide better photoprotection in the UVA region.

Zeta potential analysis indicated that lignin and nanocomposites carried a negative charge in the solvent, with LigTiO<sub>2</sub> showing greater stability in its zeta potential. This negative charge is attributed to hydroxyl functional groups in lignin. Despite lower stability, LigZnO remains within the stable range, as Ribeiro *et al.*<sup>26</sup> reported that zeta potential values |−25 mV| and |−30 mV| or more insufficient to create an energy barrier that prevents coalescence. Lignin and nanocomposites exhibited nanoscale dimensions (Supporting Information, Fig. S2). Lignin exhibited a bimodal size distribution, with two ranges: 40–70 nm and 550–1100 nm.

Lignin is recognized as a natural phenolic biopolymer. It possesses chromophore functional groups that enable it to absorb a broad spectrum of UV light, specifically in the range of 250–400 nm. Unsaturated functional groups are primarily responsible for lignin's brownish to black coloration. These

**Table 1. Yields, λ<sub>max</sub> (nm), UV A/UV B ratio, zeta potential, and size of lignin and lignin-based nanocomposites (LigZnO and LigTiO<sub>2</sub>).**

Material	Yield (%)	λ <sub>max</sub> (nm)	UVA/UVB ratio	Zeta potential (mV)	Size (nm)
Lignin	55.2 ± 2.2 <sup>a</sup>	280	1.8	−41 ± 0	56 ± 5 and 691 ± 77 <sup>b</sup>
LigZnO	37.2 ± 1.3	280	2.4	−32 ± 1	864 ± 17
LigTiO <sub>2</sub>	34.3 ± 2.2	287	2.4	−48 ± 1	789 ± 12

<sup>a</sup>Data from Serpa *et al.*<sup>12</sup>

<sup>b</sup>Means from two signals of the lignin size distribution that presented a bimodal distribution.

include conjugated carbonyl groups, aromatic rings, and carbon–carbon double bonds.<sup>27</sup>

In previous studies conducted by Serpa *et al.*,<sup>12</sup> lignin extracted from cashew apple bagasse (CAB) underwent <sup>1</sup>H–<sup>13</sup>C HSQC NMR analysis, which identified syringyl, guaiacyl, *p*-coumarate, and oxidized syringyl as the main functional groups, with a syringyl/guaiacyl ratio intensity of 0.835. This composition highlights CAB-lignin as a promising natural ingredient for sunscreen formulations.

The functional groups present in lignin and its nanocomposites (LigZnO and LigTiO<sub>2</sub>) were confirmed through FTIR spectroscopy (Fig. 1). The characteristic vibrations of lignin in the 1650–1400 cm<sup>-1</sup> range include aromatic skeletal vibrations (C=C) at 1617 cm<sup>-1</sup>, C=C stretching vibrations in phenolic rings at 1513 cm<sup>-1</sup>, and C–H deformations (CH and CH<sub>2</sub>) from phenolic rings at 1450 cm<sup>-1</sup>, which is consistent with the literature.<sup>12,28</sup>

In the LigZnO spectrum (Fig. 1b), a low-intensity signal between 450 and 400 cm<sup>-1</sup> corresponds to the stretching of ZnO.<sup>10</sup> However, the LigTiO<sub>2</sub> spectrum (Fig. 1c) displayed a high-intensity band between 400 and 900 cm<sup>-1</sup>, which is attributed to Ti–O–Ti stretching vibrations.<sup>29</sup>

The band observed at 1115 cm<sup>-1</sup> in the LigZnO spectrum is attributed to ether linkages,<sup>12</sup> and the band at 1140 cm<sup>-1</sup> indicates the presence of aromatic systems in both lignin (Fig. 1a) and LigZnO (Fig. 1b). The symmetric bending vibrations of C–H bonds in methoxyl groups of syringyl and guaiacyl units, which occur in the range of 1450–1390 cm<sup>-1</sup>,<sup>30</sup> are evident in all spectra (lignin and nanocomposites). A band around 1620 cm<sup>-1</sup>, characteristic of lignin due to

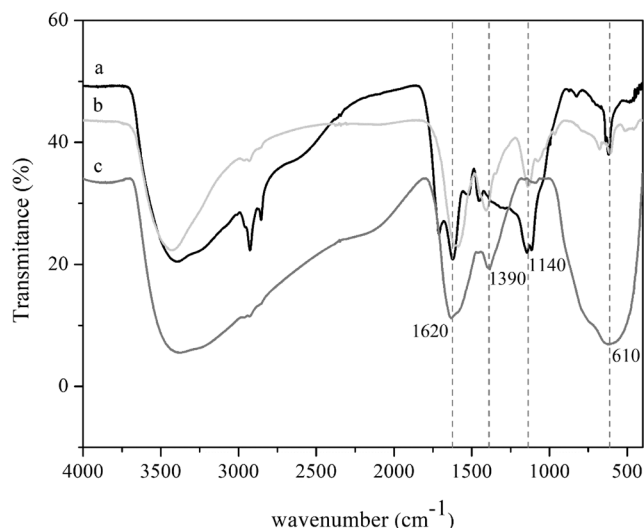


Figure 1. Fourier transform infrared (FTIR) spectra of the of lignin from cashew apple bagasse and synthesized lignin-based nanocomposites. (a) Lignin. (b) LigZnO. (c) and LigTiO<sub>2</sub>.

aromatic skeletal vibrations (C=C),<sup>30</sup> was observed in both nanocomposites (Fig. 1b,c). Notably, C=O stretching from conjugated para-substituted aryl ketones was only identified in lignin at 1640 cm<sup>-1</sup>,<sup>12</sup> and was also evident in the lignin spectrum.

X-ray diffraction was used to verify the presence of metal oxides in lignin hybrid nanocomposites. Only in the LigZnO nanocomposite (Supporting Information, Fig. S3) was it possible to detect sharp peaks in XRD indicating the presence of crystalline structures in the nanocomposite. For LigTiO<sub>2</sub> no signal was observed. The diffractograms of lignin and LigZnO show an amorphous region in the 2θ range of 20°–30°, which is characteristic of lignin. The highest signals identified in LigZnO diffractogram at 2θ of 37° (100) and 40° (002) were also observed in commercial ZnO, suggesting the presence of ZnO in the structure of the LigZnO nanocomposite.<sup>31</sup> The XRD results for the LigTiO<sub>2</sub> nanocomposite are consistent with the results obtained by Kaur *et al.*,<sup>11</sup> who also did not detect peaks in XRD for their lignin-titanium dioxide nanocomposite synthesized using commercial alkali lignin.

## Determination of the antioxidant activity and SPF of sunscreens

Table 2 shows the antioxidant properties and SPF of formulations incorporating UV-absorbers in commercial lotions (emulsion base and sunscreen). Lignin from cashew bagasse demonstrated high antioxidant potential in comparison with the other lignin-based nanocomposites. LigZnO exhibited a scavenging effect of 31.8%, similar to LigTiO<sub>2</sub> (28.9%), but commercial oxides showed lower

**Table 2. Antioxidant activity and SPF of emulsion base and sunscreen commercial lotions incorporated with lignin, lignin nanocomposites, zinc commercial oxide, or titanium commercial oxides.**

Material	Scavenging (%)	SPF (base lotion) <sup>a</sup>	SPF (sunscreen) <sup>b</sup>
Control	–	0.0 ± 0.0	12.6 ± 0.3
Lignin	94.5 ± 0.9	0.94 ± 0.0	11.9 ± 0.3
ZnO commercial	9.4 ± 1.8	1.03 ± 0.0	13.0 ± 0.6
TiO <sub>2</sub> commercial	9.2 ± 2.0	0.71 ± 0.0	13.9 ± 0.6
LigZnO	31.8 ± 1.1	0.55 ± 0.0	15.9 ± 0.3
LigTiO <sub>2</sub>	28.9 ± 1.1	1.10 ± 0.0	15.7 ± 0.5

<sup>a</sup>Formulations with 5% (w/w) of lignin, nanocomposites and commercial oxides in emulsion base lotion.

<sup>b</sup>Formulations with 5% (w/w) of lignin, nanocomposites and commercial oxides in sunscreen lotion.

effects, with ZnO at 9.4% and TiO<sub>2</sub> at 9.2%. Thus, the reduced antioxidant potential of lignin nanocomposites is consistent with the low antioxidant activity of the commercial nanoparticles.

The antioxidant activity of lignin can be attributed to the presence of phenolic groups in its structure. Adding zinc and titanium, which can interact with phenolic groups, probably reduces its availability and further decreases the scavenging effect. Although the results of lignin nanocomposites were superior to those of commercial nanoparticles, they were still inferior to the results obtained by Kaur *et al.*,<sup>10,11</sup> applying the same proportions of lignin and oxides. In this case, the lower lignin nanoparticle size used in the literature contributed to a larger nanocomposite surface area and greater availability of groups with antiradical action.

The SPF for all the formulations was calculated using absorbance data and Eqn (2). The emulsion base did not have an SPF but the commercial sunscreen had a SPF of  $12.6 \pm 0.3$ . In all formulations prepared in the base emulsion, low SPF values (0.55–1.10) were obtained, with a few increasing in SPF for LigTiO<sub>2</sub> (1.10), and a reduction for LigZnO (0.55) when compared with lignin (0.94). In the same proportions, the SPF values of the formulations incorporated with commercial oxides (0.71–1.03) were also low. The sunscreen lotion with lignin or with commercial oxides (ZnO or TiO<sub>2</sub>) incorporated had an SPF value lower than sunscreen lotions containing LigZnO or LigTiO<sub>2</sub> lignin-based nanocomposites (Table 2). The SPF values for the sunscreen lotions with these nanocomposites incorporated were similar and greater than expected based on the results obtained with the emulsion base without UV blockers. This phenomenon can be attributed to the lignin's tendency to act as a booster agent. These agents are additives that weakly absorb ultraviolet (UV) rays but enhance the effectiveness of UV filters through synergistic physical and electron transfer processes. Piccinino *et al.*<sup>24</sup> highlighted this attribute, reporting that a mixture of natural UV filters and lignin nanoparticles exhibited a synergistic UV boosting effect (BE), which was also observed in this study for lignin-based nanocomposites. The BEs in sunscreens containing LigZnO and LigTiO<sub>2</sub> were 26.2% and 24.6%, respectively, surpassing the performance of commercial oxides (3.2% for ZnO and 10.3% for TiO<sub>2</sub>) in conventional sunscreen formulations. Notably, the boosting effect was not observed with lignin alone, underscoring the significance of synthesizing nanocomposites. The formulations with lignin and lignin-based nanocomposites showed a brownish tone (Supporting Information, Fig. S3) in the emulsion base and in commercial sunscreen lotions. The formulations with lignin incorporated presented with a brown appearance whereas the formulation with LigZnO left

the lotions with a grayish-brown tone, and the incorporation with LigTiO<sub>2</sub> left the formulations with a light brown aspect. A change in appearance was observed in all formulations doped with lignin, which became more fluid. This highlights the importance of synthesizing lignin nanocomposites with zinc and titanium oxides. Rheological behavior was examined to assess the compatibility of lignin nanocomposites in an emulsion base and commercial sunscreen.

## Rheological measurements of sunscreens lotions

Dynamic rheometry assesses the physicochemical characteristics of the formulations, providing data relevant to structural changes in the product resulting from the addition of lignin-based nanocomposites. This technique enables the determination of viscoelastic properties without disrupting the internal structure of the system. In Supporting Information, Fig. S5, the results of the dynamic measurements of the elastic modulus ( $G'$ ) and the viscous modulus ( $G''$ ) are plotted for the emulsion base and commercial sunscreen obtained by the addition of the lignin, lignin-based nanocomposites or commercial oxides. According to the results, except for the commercial sunscreen only (control),  $G'$  values were greater than  $G''$  values over the period of analysis, so the energy was dissipated by elastic flow – i.e., the elastic properties predominated in relation to viscous properties. The appearance analysis of the formulations that were obtained (Supporting Information, Fig. S4), except for the formulations incorporated with lignin, indicates that gel-like structures were present in these formulations.<sup>32,33</sup>

This elastic behavior in emulsion base formulations indicates that there was no change in the original characteristics of the control (emulsion base only). On the other hand, the inversion observed in the profile of storage  $G'$  and loss  $G''$  moduli in commercial sunscreen formulations indicates that the material exhibits predominantly elastic rather than viscous characteristics. Presumably, a positive interaction between UV blockers and/or lotion components with lignin nanocomposites and commercial oxides contributes to the structure of the lotion network.

A controlled shear rate rheological analysis was conducted to examine the viscosity trends as a function of the applied shear rate (Supporting Information, Fig. S6). All formulations displayed curves with similar profiles, indicating typical shear-thinning behavior characteristic of non-Newtonian fluids. This behavior is characterized by a reduction in viscosity with increasing shear rate, and no significant changes in viscosity behavior were observed due

to the addition of nanomaterials. The viscosity curves also demonstrated the response of the colloidal system to flow. As the shear rate increases, the fluid structures are gradually disrupted, causing aggregates to align in the direction of flow (pseudoplastic flow), thereby decreasing friction and reducing viscosity.<sup>34</sup>

When analyzing the shear rate dependence of steady shear viscosity, both formulations containing lignin (5% w/w) exhibited lower absolute viscosity values in comparison with the controls (emulsion base or commercial sunscreen), indicating a loss of the formulation's physical characteristics – a notable result, particularly evident in the commercial sunscreen with lignin. These findings suggest that, under these conditions, lignin absorbs water from the sunscreen and does not contribute to the structural network of the

emulsion. This rheological characteristic is closely related to spreadability, a key property when cosmetics are applied to human skin under typical use conditions.<sup>3</sup>

Consistency can be evaluated at low shear rates and correlated with yield stress, whereas spreadability can be assessed subjectively at high shear rates and is thus associated with shear-thinning viscosity.<sup>33</sup> In this context, it can be inferred that the incorporation of lignin-based nanocomposites improved consistency without altering the spreadability of the formulations significantly in comparison with the controls (emulsion base and commercial sunscreen), while remaining compatible with commercial organic UV absorbers.

Thixotropy, an important property of non-Newtonian fluids, refers to a time-dependent 'gel-sol' interconversion

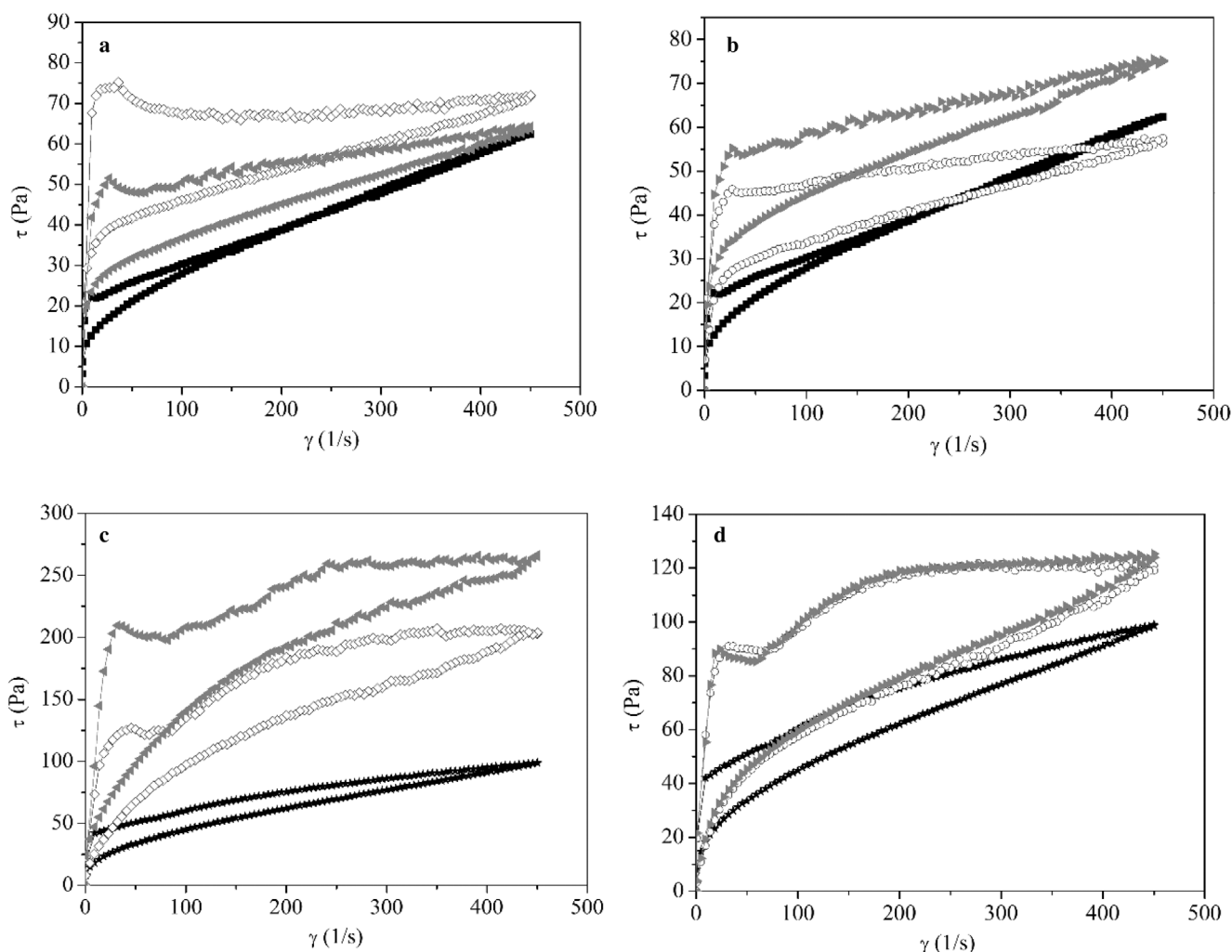


Figure 2. Rheograms of emulsion base and commercial sunscreen lotions: (a) Emulsion base containing LigZnO (◄) and ZnO (◊). (b) Emulsion base containing LigTiO<sub>2</sub> (►) and TiO<sub>2</sub> (○). (c) Commercial sunscreen containing LigZnO (◄) and ZnO (◊). (d) Commercial sunscreen containing LigTiO<sub>2</sub> (►) and TiO<sub>2</sub> (○). Emulsion base control (■) and sunscreen control (★) are included for comparison.

behavior that occurs in response to mechanical forces<sup>35</sup> and the thixotropic behavior is characterized by a reduction in structural strength during the shear load phase, followed by a relatively rapid and complete structural regeneration during the subsequent rest phase.<sup>2</sup> The rheograms (Fig. 2) of the formulations in the emulsion base (Fig. 2a,b) and in the commercial sunscreen (Fig. 2c,d), which incorporated lignin-based nanocomposites or oxides, demonstrate thixotropic behavior within the systems.

Dermal formulations should ideally show thixotropic rheological behavior. For cosmetics, this behavior affects the viscosity of products (more viscous systems adhere better to the skin) and the feeling after use. According to Keck and Schwabe<sup>5</sup> and Xiao *et al.*,<sup>36</sup> products with thixotropy are easy to spread and can be absorbed by the skin, these being important factors for cosmetics containing active substances. For formulations with lignin nanocomposites, the viscosity and the yield point were higher in comparison with the controls. Interestingly, the increase in viscosity and yield point were more pronounced for the formulation in commercial sunscreen than in the emulsion base, suggesting a positive interaction with sunscreen components. This effect can be attributed to LigZnO and LigTiO<sub>2</sub> influencing the association of the original sunscreen's UV absorbers, ethylhexyl methoxycinnamate (Parsol MCX) and butyl methoxydibenzoylmethane (avobenzone), in different ways, leading to an increase in the viscosity of the formulation.

The hysteresis area was determined from Fig. 2. The thixotropic loop areas were large in the emulsion base with incorporated LigZnO (4 kPa s<sup>-1</sup>, Fig. 2a) and LigTiO<sub>2</sub> (4 kPa s<sup>-1</sup>, Fig. 2b), as well as in commercial sunscreen with LigZnO (22 kPa s<sup>-1</sup>, Fig. 2c) and LigTiO<sub>2</sub> (14 kPa s<sup>-1</sup>, Fig. 2d). These samples exhibited strong thixotropy, exceeding that of the commercial cosmetic controls (0.4 kPa s<sup>-1</sup> for the emulsion base and 5 kPa s<sup>-1</sup> for the commercial sunscreen). This suggests a synergistic interaction between LigTiO<sub>2</sub> or LigZnO and the control lotions, reinforcing thixotropic behavior. Additionally, a positive interaction between LigZnO or LigTiO<sub>2</sub> and the commercial UV blockers and/or lotion components is indicated by the increased SPF values (Table 2) observed in the original lotion upon addition of lignin-based nanocomposites.

These results indicate that lignin derived from cashew apple bagasse (CAB) is a promising alternative for the development of UV blockers, owing to its availability, low cost, and potential to reduce the reliance on commercial organic filters. Organic filters have been associated with negative hormonal effects in animal models but no adverse effects have been confirmed in humans, although further investigations are ongoing.<sup>4</sup> In this context, the use of inorganic sunscreens has become increasingly important as an alternative for patients.

Differentiating the effects of ZnO and TiO<sub>2</sub> from naturally occurring particles presents challenges.<sup>4</sup> Although TiO<sub>2</sub> is often considered more environmentally friendly than ZnO,<sup>37</sup> further studies are required before drawing any definitive conclusions. Currently, the overall risk to the environment from these compounds is deemed extremely low, especially given that the concentrations of oxides found in the environment (10–100 µg L<sup>-1</sup> of TiO<sub>2</sub>) are significantly lower than those tested in the literature. However, the potential risks to the environment could increase if greater concentrations of inorganic filters leach into ecosystems. This remains to be investigated.<sup>4,38</sup> In this regard, lignin nanocomposites emerge as a promising alternative for reducing and/or replacing both commercial organic and inorganic UV blockers, thereby mitigating the potential environmental damage associated with their accumulation.

## Conclusions

Lignin from cashew apple bagasse has high antioxidant potential and lignin-based nanocomposites (LigZnO and LigTiO<sub>2</sub>) present high stability, a scavenging effect, and UV-blocking properties with a high UV A spectrum of protection. The addition of lignin-based nanocomposites to emulsion base and commercial sunscreen lotions promoted satisfactory stability of the cosmetic emulsion in comparison with the addition of lignin alone, based on the similar rheological properties in formulations with nanocomposites or oxides compared with controls. Thus, the formulations prepared using LigZnO and LigTiO<sub>2</sub> have strong potential for use as an additive to sunscreen for brown skin tone and are compatible with commercial UV blockers. Overall, the lignin-based nanocomposites (LigZnO and LigTiO<sub>2</sub>) promoted a boosting effect when used with commercial UV-absorbers, being capable of reducing the use of commercial organic and inorganic filters, mitigating the possible damage caused by their accumulation in the environment. The synthesis of lignin nanocomposites also helps to decrease cashew apple bagasse disposal problems while lignin is valorized simultaneously.

## Acknowledgements

We are grateful to Embrapa Agroindústria Tropical for the support of the infrastructure in carrying out analyses of the characterization of nanocomposites and rheological properties. We also acknowledge the Brazilian research funding institutions, Fundação Cearense de Apoio ao Desenvolvimento Científico e Tecnológico (FUNCAP)

and Conselho Nacional de Desenvolvimento Científico e Tecnológico (CNPq). The Article Processing Charge for the publication of this research was funded by the Coordenação de Aperfeiçoamento de Pessoal de Nível Superior - Brasil (CAPES) (ROR identifier: 00x0ma614).

## Funding information

This work was supported by Fundação Cearense de Apoio ao Desenvolvimento Científico e Tecnológico – FUNCAP (grant number BP4-00172-00122.01.00/20), and Conselho Nacional de Desenvolvimento Científico e Tecnológico – CNPq (grant numbers 405840/2022-5 and 316373/2021-4).

## Conflict of interest statement

The authors declare no competing interests.

## References

- Ma Y and Yoo J, History of sunscreen: An updated view. *J Cosmet Dermatol* **20**:1044–1049 (2021).
- Ferrari M and Rocha-Filho PA, Multiple emulsions containing amazon oil: Açaí oil (*Euterpe oleracea*). *Rev Bras Farmacogn* **21**:737–743 (2011).
- Tafuro G, Costantini A, Baratto G, Francescato S, Busata L and Semenzato A, Characterization of polysaccharidic associations for cosmetic use: Rheology and texture analysis. *Cosmetics* **8**:1–17 (2021).
- Schneider SL and Lim HW, A review of inorganic UV filters zinc oxide and titanium dioxide. *Photodermatol Photoimmunol Photomed* **35**:442–446 (2019).
- Xiao Q, Chen G, Zhang YH, Chen FQ, Weng HF and Xiao AF, Agarose stearate-carbomer<sub>940</sub> as stabilizer and rheology modifier for surfactant-free cosmetic formulations. *Mar Drugs* **19**:1–24 (2021).
- EWG's Sunscreen Guide, EWG's 18th annual guide to sunscreens Available: <https://www.ewg.org/sunscreen/report/executive-summary/#.wxcjvvmvxb> [accessed 29 October 2023].
- Kaur R, Sanjeev K, Bhardwaj SC, Kim KY and Bhaumik J, Lignin-based metal oxide nanocomposites for UV protection applications: A review. *J Clean Prod* **317**:1–11 (2021).
- Zhang Y and Naebe M, Lignin: A review on structure, properties, and applications as a light-colored UV absorber. *ACS Sustain Chem Eng* **9**:1427–1442 (2021).
- Widsten P, Lignin-based sunscreens—state-of-the-art, prospects and challenges. *Cosmetics* **7**:1–8 (2020).
- Kaur R, Thakur NS, Chandna S and Bhaumik J, Development of agri-biomass based lignin derived zinc oxide nanocomposites as promising UV protectant-cum-antimicrobial agents. *J Mater Chem B* **8**:260–269 (2020).
- Kaur R, Thakur NS, Chandna S and Bhaumik J, Sustainable lignin-based coatings doped with titanium dioxide nanocomposites exhibit synergistic microbicidal and UV-blocking performance toward personal protective equipment. *ACS Sustainable Chem Eng* **9**:11223–11237 (2021).
- Serpa JF, Silva JS, Reis CLB, Micoli L, Silva LMA, Canuto KM *et al.*, Extraction and characterization of lignins from cashew apple bagasse obtained by different treatments. *Biomass Bioenergy* **141**:1–11 (2020).
- Girão Neto CAC, Prasilde ICM, da Silva AS, Silva LMA, Canuto KM, Fontenelle ROS *et al.*, Enzymatic synthesis of citronellyl butyrate by lipase B from *Candida antarctica* immobilized on magnetic cashew apple bagasse lignin. *Process Biochem* **131**:244–255 (2023). <https://doi.org/10.1016/j.procbio.2023.06.025>.
- Paul R, Kalita P, Wong BM and Mondal J, Progress and outlook of solar-powered biomass for biorefineries: A minireview. *Energy Fuel* **36**:14573–14583 (2022).
- de Albuquerque TL, Gomes SDL, Marques Júnior JE, da Silva IJ and Rocha MVP, Xylitol production from cashew apple bagasse by *Kluyveromyces marxianus* CCA510. *Catal Today* **255**:33–40 (2015). <https://doi.org/10.1016/j.cattod.2014.10.054>.
- de Albuquerque TL, Gomes SDL, Marques Júnior JE, de Queiroz LP, Ricardo ADS and Rocha MVP, Polylactic acid production from biotechnological routes: A review. *Int J Biol Macromol* **186**:933–951 (2021). <https://doi.org/10.1016/j.ijbio.2021.07.074>.
- Rodrigues THS, de Barros EM, Brígido JS, da Silva WM, Rocha MVP and Gonçalves LRB, The bioconversion of pretreated cashew apple bagasse into ethanol by SHF and SSF processes. *Appl Biochem Biotechnol* **178**:1167–1183 (2016).
- Silva JS, Mendes JS, Correia JAC, Rocha MVP and Micoli L, Cashew apple bagasse as new feedstock for the hydrogen production using dark fermentation process. *J Biotechnol* **286**:71–78 (2018).
- Rocha MVP, Rodrigues THS, de Macedo GR and Gonçalves LRB, Enzymatic hydrolysis and fermentation of pretreated cashew apple bagasse with alkali and diluted sulfuric acid for bioethanol production. *Appl Biochem Biotechnol* **155**:407–417 (2009).
- Mansur JS, Breder MNR, Mansur MCA and Azulay RD, Determination of sun protection factor by spectrophotometry. *An Bras Dermatol* **61**:121–124 (1986a).
- Mansur JS, Breder MNR, Mansur MCA and Azulay RD, Correlation between the determination of sun protecting of factor in human beings and by spectrophotometry. *An Bras Dermatol* **61**:167–172 (1986b).
- Gagosian VSC, Claro FC, Schwarzer ACAP, Cruz JV, Thá EL, Trindade ES *et al.*, The potential use of kraft lignins as natural ingredients for cosmetics: Evaluating their photoprotective activity and skin irritation potential. *Int J Biol Macromol* **222**:2535–2544 (2022).
- Sayre RM, Agin PP, Levee GJ and Marlowe E, Comparison of in vivo and in vitro testing of sunscreens formulas. *Photochem Photobiol* **29**:559–566 (1979).
- Piccinino D, Capecchi E, Delfino I, Crucianelli M, Conte N, Avitabile D *et al.*, Green and scalable preparation of colloidal suspension of lignin nanoparticles and its application in eco-friendly sunscreen formulations. *ACS Omega* **6**:21444–21456 (2021).
- Donglikar MM and Deore SL, Development and evaluation of herbal sunscreen. *Pharm J* **9**:83–97 (2017).
- Ribeiro RCA, Barreto SMAG, Ostrosky EA, Rocha-Filho PA, Verissimo LM and Ferrari M, Production and characterization of cosmetic nanoemulsions containing *Opuntia ficus-indica* (L.) Mill extract as moisturizing agent. *Molecules* **20**:2492–2509 (2015).
- Sadeghifar H and Ragauskas A, Lignin as a UV light blocker – A review. *Polymers* **12**:1–10 (2020).

28. Reis CLB, Silva LMA, Rodrigues THS, Félix AKN, de Santiago-Aguiar RS, Canuto KM *et al.*, Pretreatment of cashew apple bagasse using protic ionic liquids: Enhanced enzymatic hydrolysis. *Bioresour Technol* **224**:694–701 (2017). <https://doi.org/10.1016/j.biortech.2016.11.019>.
29. Li Y, Yang D, Lu S, Qiu X, Qian Y and Li PW, Encapsulating TiO<sub>2</sub> in lignin-based colloidal spheres for high sunscreen performance and weak photocatalytic activity. *ACS Sustainable Chem Eng* **7**(6):6234–6242 (2019). <https://doi.org/10.1021/acssuschemeng.8b06607>.
30. Lopes AMC, João KG, Rubik DF, Bogel-Lukasik E, Duarte LC, Andreus J *et al.*, Pre-treatment of lignocellulosic biomass using ionic liquids: Wheat straw fractionation. *Bioresour Technol* **142**:198–208 (2013).
31. Marouf S, Beniaiche A, Guessas H and Azizi A, Morphological, structural and optical properties of ZnO thin films deposited by dip coating method. *Mater Res* **20**:88–95 (2017).
32. Tadros T, Application of rheology for assessment and prediction of the long-term physical stability of emulsions. *Adv Colloid Interface Sci* **108/109**:227–258 (2004).
33. Kwak MS, Ahn HJ and Song KW, Rheological investigation of body cream and body lotion in actual application conditions. *Korea Aust Rheol J* **27**:241–251 (2015).
34. Tafuro G, Costantini A, Baratto G, Busata L and Semenza A, Rheological and textural characterization of acrylic polymer water dispersions for cosmetic use. *Ind Eng Chem Res* **58**:23549–23558 (2019).
35. Wei YX, Lin YB, Xie R, Xu YF and Yao J, The flow behavior, thixotropy and dynamical viscoelasticity of fenugreek gum. *J Food Eng* **166**:21–28 (2015).
36. Keck CM and Schwabe K, Silver-nanolipid complex for application to atopic dermatitis skin: Rheological characterization, in vivo efficiency and theory of action. *J Biomed Nanotechnol* **5**:428–436 (2009).
37. Corinaldesi C, Marcellini F, Nepote E, Damiani E and Danovaro R, Impact of inorganic UV filters contained in sunscreen products on tropical stony corals (*Acropora* spp.). *Sci Total Environ* **638**:1279–1285 (2018).
38. Hanigan D, Truong L, Schoepf J, Nosaka T, Mulchandani A, Tanguay RL *et al.*, Trade-offs in ecosystem impacts from nanomaterial versus organic chemical ultraviolet filters in sunscreens. *Water Res* **139**:281–290 (2018).



#### Tigressa Helena Soares Rodrigues

Tigressa Helena Soares Rodrigues holds a PhD in chemical engineering with a focus on chemical and biochemical processes. She is a professor at Universidade Estadual Vale do Acaraú, Ceará State, Brazil, where her research focuses

on biotechnology, particularly the bioprospecting of bioactive compounds and the development of bioprocesses for the utilization and valorization of residual biomass.



#### Gabriel Arcanjo Bezerra Matias

Gabriel Arcanjo Bezerra Matias graduated in chemical engineering, with an emphasis on industrial processes. He has experience in the study of bioprocesses to add value to waste from industrial biomass processing.



#### Vanessa Moreira Frota

Vanessa Moreira Frota holds a bachelor's degree in chemistry and a technical qualification in agroindustry. She is currently a master's student in chemical engineering at the Federal University of Ceará, Ceará State, Brazil, and a post-junior

advisor at Alquimista Júnior Soluções Químicas. Her research focuses on natural product chemistry and biotechnological processes, particularly the development of new products from residual agroindustrial biomass.



#### Adriano L. A. Mattos

Adriano L. A. Mattos holds a PhD in materials science and engineering. He is currently an analyst at the Brazilian Agricultural Research Company. His expertise lies in nonmetallic materials

engineering with a focus on the characterization and processing of polymers, biopolymers, and composite materials.



#### Maria Valdez Ponte Rocha

Maria Valdez Ponte Rocha holds a PhD in chemical engineering and is a professor at the Federal University of Ceará, Ceará State, Brazil. Her research focuses on biochemical processes, including the biotechnological production of biosurfactants, first- and

second-generation ethanol, biohydrogen, xylitol, aromas, and enzymes. She specializes in utilizing agroindustrial waste, particularly from the cashew industry, and the study of petroleum bioremediation processes.